

Radiation safety design of super KEKB factory

Toshiya Sanami

High Energy Accelerator Research Organisation (KEK), Japan

Abstract

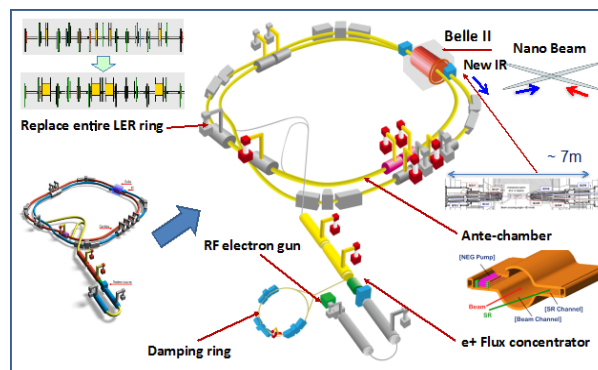
The SuperKEKB factory, which was scheduled to start operation early 2015, is an electron-positron collider designed to produce an 80×10^{34} -1/cm²/s luminosity, which is 40 times greater than the KEKB factory. Built to investigate CP violation and “new physics” beyond the Standard Model, the facility consists of a 7-GeV electron/3.5-GeV positron linac, a 1.1-GeV positron damping ring, beam transport, and a 7-GeV electron/4-GeV positron collider. To meet this level of luminosity, the collider will be operated with a small beam size and a large crossing angle at the interaction point. According to particle tracking simulations, beam losses under these conditions will be 35 times more than those previously operated. To help optimise shielding configurations, leakage radiation and induced activity are estimated through empirical equations and detailed Monte-Carlo simulations using MARS15 code for the interaction region, beam halo collimators, emergency pathways, ducts, forward direction tunnels, and positron production target. Examples of shielding strategies are presented to reduce both leakage dose and airborne activity for several locations in the facility.

Introduction

The SuperKEKB factory – an electron-positron collider – is designed to produce a luminosity of 80×10^{34} 1/cm²/s, 40 times greater than its predecessor, the KEKB factory. Built to investigate CP violation and “new physics” beyond the Standard Model [1], the facility consists of a 7-GeV electron/3.5-GeV positron linac, a 1.1-GeV positron damping ring, beam transport, and a 7-GeV electron/4-GeV positron collider. To attain this luminosity, the collider will operate with a small beam size and a large crossing angle at the interaction point. According to particle tracking simulations, beam losses under these conditions will be 35 times more than those previously given. Leakage radiation and induced activity are estimated through empirical equations and detailed Monte-Carlo simulations using MARS15 for the interaction region, beam halo collimators, emergency pathways, ducts, forward direction tunnels and positron production target, to aid shield design optimisation.

This paper describes examples of shielding strategies used to reduce both leakage dose and concentration of airborne activity around several parts of the facility.

Figure 1. Schematic drawing of the super KEKB factory



Design specifications

Figure 1 shows a schematic of the SuperKEKB factory, together with a device upgrade plan. The SuperKEKB factory uses a 3-km-long circular tunnel, at a depth of 10 m underground. The ring has four straight and four curved sections. Three of the straight sections have RF cavities to accelerate the electrons and positrons; the fourth is designated as the interaction region (IR) where particle collisions take place.

To achieve higher luminosity, various hardware devices were replaced, including the electron gun, the flux concentrator to enhance positron production, the 3-km-long beam chamber, and the magnets of the low energy ring (LER) for positrons, and an upgrade in IR design and for the detector (Belle2). A damping ring was newly installed to improve the positron beam emittance.

Table 1 lists the design specifications for the SuperKEKB factory along with those of the previous KEKB factory for comparison. SuperKEKB commissioning will proceed in three stages, named phases 1–3. Phase-1 operations will start in 2015 with vacuum scrubbing and injection beam tuning. On completion of phase 1, phase 2 will start with collision tuning, the Belle2 detector with operations, anticipated to begin within 5 months. Phase 3 operations will then start with a physics run. The target luminosity in phase 3 is 80×10^{34} 1/cm²/s, which is 80 times greater than the design value for the KEKB factory.

Table 2 summarises beam loss estimations obtained from particle tracking simulations. Beam losses are caused by three processes, namely beam-gas interaction, radiative-Bhabha, and Touschek. Beam-gas interaction occurs between the remaining gas molecules and circulating beam particles. It is roughly proportional to the beam current and the level of vacuum. Beam loss from radiative-Bhabha originates from energy losses from electron-positron interactions at the interaction point; the amount is proportional to luminosity.

Beam loss from Touschek stems from scattering within the bunches of the beam, and is related to beam size. From KEKB to SuperKEKB, all three losses will increase because of the increases in the beam current and luminosity, and the decreased beam size.

Table 1. Design specifications for the KEKB and SuperKEKB

	KEKB	SuperKEKB phase1	SuperKEKB phase1	SuperKEKB phase2
Beam energy and current	LER 3.5 GeV/2.9 A HER 8 GeV/1.2 A	LER 4 GeV/1 A HER 7 GeV/1 A	LER 4 GeV/1.8 A HER 7 GeV/1.3 A	LER 4 GeV/3.6 A HER 7 GeV/2.6 A
Target luminosity	1x10 ³⁴	0	1x10 ³⁴	80x10 ³⁴
Duration	11 years from 1998	5 months from 2015	5 months after 9-month shut-down (Belle2 install)	After 3-month shut-down (VXD install)
Operation mode	Physics run	Injection tuning Vacuum scrubbing without Belle2	Collision tuning with limited number of cavities, without VXD	Physics run

As shown in Table 2, beam loss increases step-by-step with increasing beam current and luminosity. In phase 3, the total number of particles lost from the beam is over 30 times greater than for KEKB. Finally, the total beam loss power rises to nearly 500 W. Secondary radiation should be shielded properly to mitigate radiation leakage and lower the concentration of airborne activity.

Table 2. Beam losses at KEKB and SuperKEKB

unit [10 ⁹ pps]	Beam life				Injection and abort	Total
	Ring uniform (Beam gas)	Arc uniform (Touschek)	Collimator local	IR RBB		
LER HER						
KEKB	0.53 0.01	0.98 0.65	5.44 0.71	1.43 1.44	15.2 6.12	24 9
Super KEKB Phase1	4.36 0.937	0 0	0 0	0 0	4.68 3.86	9 5
Super KEKB Phase2	16.95 0.67	31.25 31.30	233.5 80.0	1.13 0.83	69.1 24.9	351 138
Super KEKB Phase3	33.90 1.33	62.5 62.6	467.0 160.0	90.4 66.2	138 49.8	792 340

Airborne activity and leakage dose using empirical equations

From the beam loss estimations listed in Table 2, induced air activity and leakage dose were deduced using empirical equations. Our goal in shielding design was for less than 20 µSv/h for controlled areas, 1.5 µSv/h for the supervised areas, and 0.2 µSv/h for general areas. Concentrations of airborne activity should be less than the limits for release air that are determined according to chemical composition.

For estimation of airborne activities, Swanson's specific activity was used with a 2-m average path length of above 20 MeV photon in air. Beam losses at dumps were not taken into account for this estimation because electron/positron powers are fully absorbed within them. Sixteen air condition units (two units for each section) were assumed for this estimation. Table 3 lists typical results for the ratio of the estimated concentration of

airborne activity to the release limit, DAQpa, for air conditioning units in the curved and straight sections, and IR. The concentration of airborne activity was obtained using the saturated activity for ^3H , ^7Be , ^{11}C , ^{13}N , ^{15}O , ^{41}Ar [2] and their limits. The table contains the ratios for when the collimators are totally shielded (shown in the last row, "Phase3 WO col."). The values are useful in revealing how much reduction there is when shielding against radiation leakage is placed around the collimators.

As shown in the results, releasing air from the curved sections is difficult even with the collimators perfectly shielded. Such releases are only possible in the straight sections. To achieve this scenario, we need to consider collimator shielding.

For the IR, the concentration of airborne activity can exceed the release limit because of the large beam loss from radiative-Bhabha.

Table 3. Ratio of the estimated concentration of airborne activity to the release limit (DAQpa)

	Arc	Straight	IR
KEKB	0.56	0.02	0.07
Phase1	0.05	0.02	0.02
Phase2	8.43	0.51	1.10
Phase3	16.83	1.17	8.96
Phase3 WO col.	1.89	0.44	7.20

Table 4. Estimated dose rates on the floor of the IR experimental hall

	L side	R side
KEKB	0.12 $\mu\text{Sv/h}$	0.17 $\mu\text{Sv/h}$
Phase1	0.01 $\mu\text{Sv/h}$	0.05 $\mu\text{Sv/h}$
Phase2	0.15 $\mu\text{Sv/h}$	0.64 $\mu\text{Sv/h}$
Phase3	9.37 $\mu\text{Sv/h}$	40.3 $\mu\text{Sv/h}$

Leakage dose was estimated using Jenkins formula for the bulk shielding wall [3]. Mao's equation [4] with transfer rate obtained by a Monte Carlo N -particle calculation [5] was used for the duct-streaming problem. The skyshine radiation dose at the site boundary was estimated using the Thomas equation [6].

Table 4 summarises estimated dose rates on the floor of the IR experimental hall for both sides of the detector. As many users would like to access the hall during beam operations, the dose rate must be below the supervised-area limit of 1.5 $\mu\text{Sv/h}$. According to beam loss scenarios, radiative-Bhabha beam loss is a contributing factor to dose rates. Additional shielding should be placed to mitigate the dose rate increase.

Detailed Monte-Carlo simulations

As shown in previous sections, additional shielding should be considered against beam losses from the collimators and the IR hall. For this purpose, three-dimensional Monte-Carlo simulations were performed using MARS15 code [7,8]. An extended geometry description, GEOM.INP, was used to configure the IR hall, tunnel, detector, and beam line devices such as chamber, magnet, and collimator.

Figure 2 shows the plan view of the beam line model in IR hall for simulations. The straight section including the IR hall has nine collimator losses and one radiative-Bhabha loss. To simulate the collimator losses, their structure and material, i.e. a 5-mm Ta tip head supported by a copper block, were modelled. For radiative-Bhabha losses, energy and particle counts from beam loss obtained from tracking simulations were embedded in a user routine of the MARS code. The electron and positron beams were injected with a 1-mrad grazing angle onto the collimator tip and inner surface of the beam pipe. Beam chamber, dipole and quadrupole magnets were modelled and placed to consider their effect.

Separated runs for each collimator and radiative-Bhabha beam losses were performed to identify the largest contribution of beam loss to the IR hall. The results showed that radiative-Bhabha in the positron ring gives the largest contribution.

Figure 2. Beam line, detector and the IR hall model for simulation

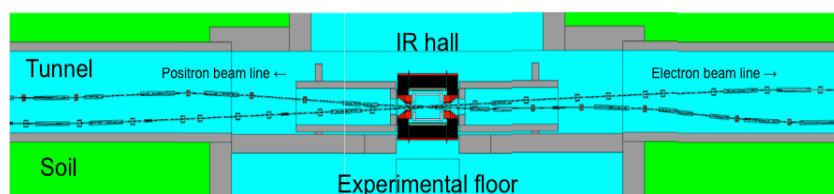


Figure 3 shows the plan view of the IR hall and the calculation result of dose rates under the original condition. Three leakage paths inducing airborne radioactivity and dose rate increases in the IR hall floor were identified: (1) un-shielded radiation along the beam duct, (2) directly through the machine-detector interface, and (3) indirectly through the gap between the tunnel and the IR hall. Four supplemental shields/modifications were designed to suppress dose rates and airborne activity on the IR hall floor; these are: (1) Lead cover surrounding the beam chamber to stop photons; (2) extended wall to completely cover the machine-detector interface part; (3) concrete and polyethylene caps to close small gaps around the detector; and (4) extended wall to cover the gap between the tunnel and the IR hall. Figure 4 shows the plan view of the IR hall and the calculation result of dose rate with the updated geometry. Dose rates on the IR hall floor were reduced to less than 1 $\mu\text{Sv/h}$, which would allow access to supervised areas.

In addition, to mitigate skyshine doses at the site boundary, additional 45-cm-thick concrete on top of the concrete shields covered the beam lines.

For collimator loss, the same methodology was followed to reduce airborne activity. Figure 5 shows the plan view for simulations of the beam-line model including a collimator. The collimator, beam pipes, and magnets were modelled to describe the spread of secondary radiation in downstream air. The total length of the beam line was 40 m.

Figure 3. Plan view of the IR hall (left) and the calculation result of dose rate (right) with original condition

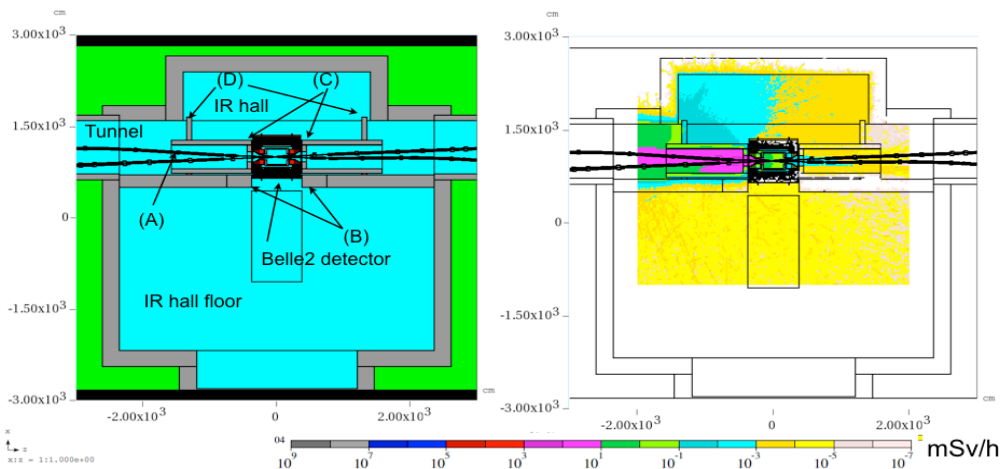
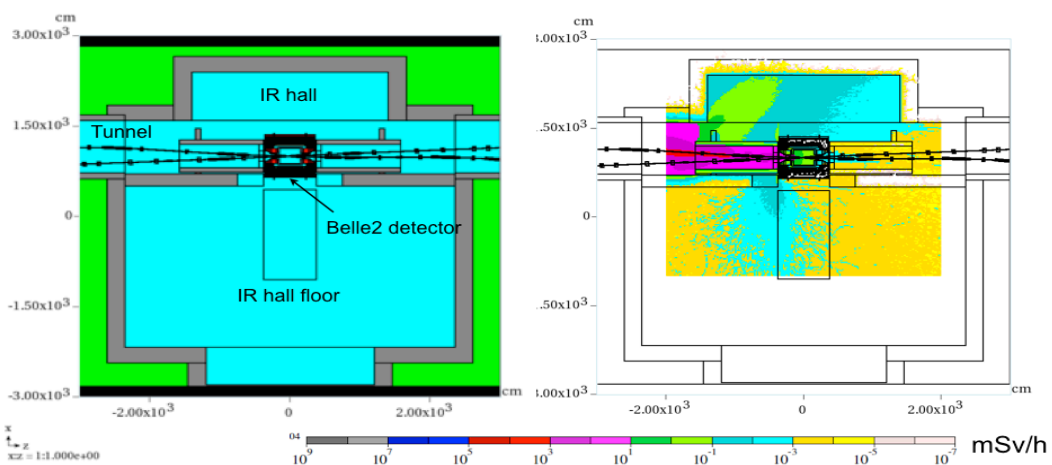


Figure 4. Plan view of the IR hall (left) and the calculation result of dose rate (right) with updated condition



The electron and positron beams were injected onto the collimator tip with 1-mrad grazing angle. All radiation produced was transported down to 20 MeV, which is close to the reaction threshold for airborne activity generation, except for ⁴¹Ar.

Figure 6 shows calculation results for a photon flux of energies above 20 MeV for the original design (upper panel) and with supplemental shield (lower panel) composed of 5-cm lead around the beam line. From the upper panel, a significant photon passes through the air. In contrast, a reduction of order greater than two in magnitude is seen in the result with lead (lower panel). Further work is required to optimise the lead block thickness and length covered ahead of beam-line maintenance work.

Figure 5. Beam line model of collimator for simulation

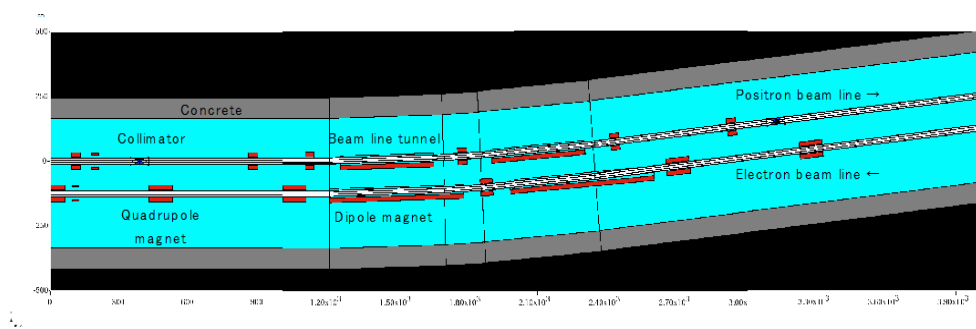
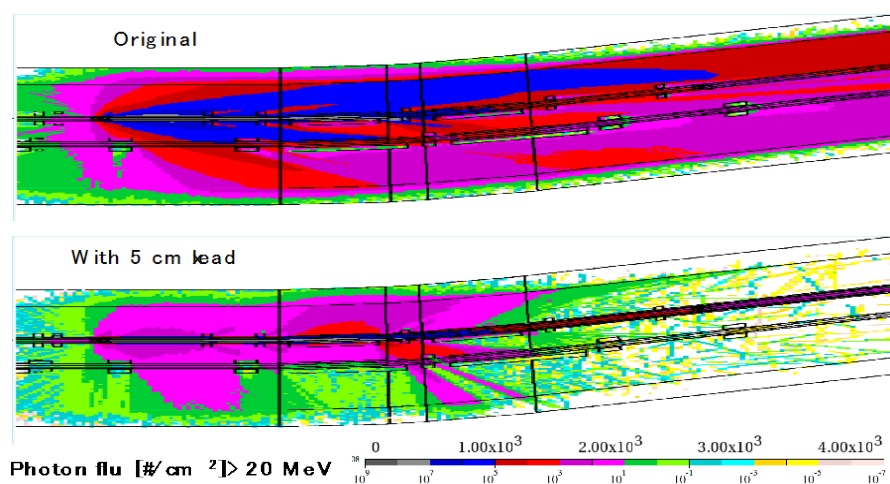


Figure 6. Photon flux above 20 MeV for original configuration and with 5 cm lead



Conclusion

Following beam loss scenarios calculated from beam tracking simulations, various radiation safety designs at the SuperKEKB factory are being developed. Bulk shield thickness and concentrations of airborne activity were estimated along the entire ring and in the IR hall. To design supplemental shielding, several locations in accessible areas, which could exceed legal limits in regard to airborne activity and dose rate, were modelled in a detailed Monte Carlo study. The supplemental shields reduced both activity and dose, however, further work is required to optimise their configurations.

References

- [1] Y. Ohnishi et al. (2013), "Accelerator design at SuperKEKB", *Prog. Theor. Exp. Phys.* 03A011.
- [2] W.P.Swanson (1979), "Radiological safety aspects of the operation of electron linear accelerators", IAEA technical reports series No.188.
- [3] T.M.Jenkins (1979), *Nucl.Instrm.Meth.* 159, 265.
- [4] X. Mao, K. Kase, W.R.Nelson (1996), *Health Phys.* 70, 207.
- [5] MGNP-A general Monte-Carlo N-Particle Transport Code Version 4A (1993), J.F.Briesmeister Ed., LA-12625-M Manual.

- [6] N.V. Mokhov (2003), "Status of MARS Code", Fermilab-Conf-03/053.
- [7] N.V. Mokhov, K.K. Gudima, C.C. James, et al. (2004), "Recent Enhancements to the MARS15 Code", Fermilab-Conf-04/053; <http://www-ap.fnal.gov/MARS/>.